Cerebello-Basal Ganglia Networks and Cortical Network Global Efficiency

T. Bryan Jackson[a], Jessica A. Bernard[a,b]

[a]Department of Psychological and Brain Sciences, Texas A&M University

[b]Texas A&M Institute for Neuroscience, Texas A&M University

Corresponding author:

T. Bryan Jackson

Department of Psychological and Brain Sciences

Texas A&M University, 4235 TAMU

College Station, TX 77843

Email: bjackson@tamu.edu

Acknowledgements

Portions of this research were conducted with the advanced computing resources provided by Texas A&M High Performance Research Computing.

Funding information: National Institute on Aging, Grant/Award Number: R01AG064010-01

Abstract

The cerebellum (CB) and basal ganglia (BG) each have topographically distinct functional subregions that are functionally and anatomically interconnected with cortical regions through discrete thalamic loops and with each other via disynaptic connections, with previous work detailing high levels of functional connectivity between these phylogenetically ancient regions. It was posited that this CB-BG network provides support for cortical systems processing, spanning cognitive, emotional, and motor domains, implying subcortical network measures are strongly related to cortical network measures (Bostan & Strick, 2018); however, it is currently unknown how network measures within distinct CB-BG networks relate to cortical network measures. Here, 122 regions of interest comprising cognitive and motor CB-BG networks and 7 canonical cortical resting-state were used to investigate whether the integration (quantified using global efficiency, GE) of cognitive CB-BG network (CCBN) nodes and their segregation from motor CB-BG network (MCBN) nodes is related to cortical network GE and segregation in 233 non-related, right-handed participants (Human Connectome Project-1200). CCBN GE positively correlated with GE in the default mode, motor, and auditory networks and MCBN GE positively correlated with GE in all networks except the default mode and emotional. MCBN segregation was related to MN segregation. These findings highlight the CB-BG network's role in executive function, task switching, and verbal working memory. This work has implications for understanding cortical network organization and cortical-subcortical interactions in healthy adults and may help in deciphering subcortical differences seen in disease states.

Keywords: cerebellum; basal ganglia; global efficiency; segregation; fMRI; Human Connectome Project

Cerebello-Basal Ganglia Networks and Cortical Network Global Efficiency

Until recently, the cerebellum (CB), basal ganglia (BG), and their networks have been relatively understudied outside of the realms of motor behavior and learning. However, the CB, BG, and their associated computations support a wide array of animal behaviors that are associated with cortical function, including human verbal, emotional, and cognitive abilities (Chen & Desmond, 2005; Guell et al., 2018; for reviews, see Ward et al., 2013 and Schmahmann, 2019). Thought to independently modulate cortical processes, the CB is associated with prediction and error-correcting processes (reviewed in Wolpert et al., 2011), while the BG is typically associated with reward and reinforcement-learning processes (reviewed in Lee, Seo, & Jung, 2012). Non-human primate studies have detailed the separate, closed-loop, trans-thalamic pathways required for this long-range communication connecting the CB and BG with the cortex and, indirectly, with each other (Kelly & Strick, 2003, 2004). However, more recent studies have revealed a direct, subcortical connection between the CB and the BG (Bostan et al., 2010; Hoshi et al., 2005). Here, we provide evidence of a highly integrated and distinct CB-BG functional networks and investigate their role in scaffolding cortical networks.

The CB and BG are phylogenetically ancient (Bell, 2002; Grillner & Robertson, 2016; Herrick M.D., 1924; Smeets et al., 2000; Stephenson-Jones et al., 2012) and throughout mammalian evolution, the CB scaled in size with the neocortex, though this increase in volume was not uniform across the structure. CB volume in great apes and humans is increased relative to neocortical volume (Barton & Venditti, 2014), with posterior CB (Crus I and Crus II) volume showing the most expansion (Balsters et al., 2010). Importantly, the posterior CB has dense projections to prefrontal regions (Ramnani et al., 2006) and has been associated with cognition in humans (Argyropoulos et al., 2020; Balsters et al., 2013; Balsters & Ranganath, 2008; King et al.,

2019; Schmahmann, 2019; Stoodley & Limperopoulos, 2016). Likewise, primate BG regions are volumetrically larger in relation to the neocortex when compared to insectivores and other earlier mammals (Stephan & Andy, 1964). This is particularly evident in the striatum, which is known to be anatomically and functionally linked with regions of the cortex associated with higher-order processing (i.e. dorsolateral prefrontal cortex) in humans (Di Martino et al., 2008; Draganski et al., 2008). With these expansions in mind, cortically-associated cognitive processing seems to be linked to CB and BG evolution (Bostan & Strick, 2018) likely via concurrent cortical expansion; however, direct investigations of the relationships between CB-BG network and cortical network interactions within healthy subjects remain rare. Specifically, Bostan and Strick (2018) have suggested that the CB and BG may provide a foundation for the evolution of these cortical networks.

The discovery of anatomical bidirectional subcortical circuits in non-human primates provides a method of communication for and supports the concept of a CB-BG network (Bostan et al., 2010; Hoshi et al., 2005). Evidence from *in vivo* human studies parallel these findings. For example, motor-associated CB and BG nodes (e.g. Lob V and Lob VI of the CB; dorsal caudal and rostral putamen of the BG) are functionally connected with one another at rest; while cognition-associated regions of the CB and BG (e.g. Crus I, Crus II, and Lob VI of the CB; inferior and superior ventral striatum, dorsal caudate, and ventral rostral putamen of the BG) are likewise functionally connected with one another at rest (Hausman, Jackson, Goen, & Bernard, 2019). Diffusion tractography (Pelzer et al., 2013), viral tract tracing (Bostan et al., 2010), and human functional connectivity (Bernard et al., 2012, 2013) studies suggest that CB-BG communication does not only exclusively rely on indirect communication via the separate, bi-directional trans-thalamic loops (Kelly & Strick, 2003, 2004). Instead, perhaps the CB and BG are part of an

anatomically and functionally integrated network that evolved to support cortical processes, including cognition in humans (Bostan & Strick, 2018).

Insights from across both neurological and psychiatric disease states support the potential importance of effective CB-BG integration. Many BG-related disorders display differences in the CB and its networks, including Parkinson's disease (Caligiore et al., 2016; DeLong & Wichmann, 2010; Wu & Hallett, 2013), dystonia (Argyelan et al., 2009; Neychev et al., 2008), and resting tremors (e.g., Asanuma, 2006). Those with schizophrenia show differences in both the CB and its networks (Anticevic et al., 2014; Ji et al., 2019; Mavroudis et al., 2017) and dopaminergic circuits within the BG (Mehler-Wex et al., 2006), and hypokinetic movements were associated with changes in CB-motor cortex connectivity (Walther et al., 2017). Even in healthy aging, there are differences in the CB-BG circuit (Hausman et al., 2019) and within the closed-loop cortico-thalamo circuits of both the CB and BG (Bernard et al., 2013; Bo et al., 2014; Griffanti et al., 2018). These findings suggest that the CB-BG network and cortical loops are important to normal function and alterations may contribute to psychiatric disorders and dysfunction.

Given the phylogenetic age of the CB and BG and their involvement in multiple cortical networks and disease states, it has been posited that these regions may provide scaffolding for cortical networks (Bostan & Strick, 2018). fMRI provides a useful way to look at intrinsic brain organization and has implications for understanding function (Karahanoğlu & Van De Ville, 2017). Resting-state fMRI was used to determine networks of functionally-connected regions that largely overlap with task positive networks that are engaged during intentional behavior (e.g. cingulo-opercular network – CON; fronto-parietal network - FPN; Fair et al., 2009) or during self-directed thought and internal mentation (i.e. the default mode network, DMN; Buckner et al., 2008; Fair et al., 2009; Fox et al., 2015). We posit that if cortical networks are supported by CB-BG

interactions, then how easily information travels within a CB-BG network (the degree of integration/interconnectedness) may be associated with information travel within cortical functional networks.

Graph theoretical approaches are useful in quantifying connectivity patterns and thus determining a given network. To quantify network integration, we calculated network-level global efficiency (GE) for both a cognitive and a motor CB-BG network and 7 canonical resting-state networks. GE is a graph theory metric defined as the average inverse shortest path length and was designed to capture the efficiency of information transmission within a given network (Rubinov & Sporns, 2010; Sporns et al., 2004; Whitfield-Gabrieli & Nieto-Castanon, 2012). It is currently unknown how CB-BG GE relates to cortical network GE; however, we hypothesized that the CB and BG each provide a foundation for cortical processing, consistent with the assertions of Bostan and Strick (2018), and thus predicted that CB-BG resting-state network-level GE would correlate positively with the GE of domain-specific cortical networks. Specifically, we predicted that cognitive CB-BG network (CCBN) GE would positively correlate with cognitive network (FPN, CON, and DMN) GE, while motor CB-BG network (MCBN) GE would be positively correlated with motor (MN) and sensory network (visual – VN, auditory – AN) GE. Previous work associated CB Lob V and Lob VI with emotional processes (Riedel et al., 2015). We further predicted a positive correlation between the MCBN GE and emotional network (EN) GE. We were also interested in network segregation (Chan et al., 2014). Segregation as a measure quantifies how disconnected nodes are from the global network. Given the hypotheses that CB-BG networks support cortical networks (Bostan & Strick, 2018), we predicted that CCBN segregation would correlate positively with FPN, CON, and DMN segregation and MCBN segregation would correlate positively with VN, AN, EN and MN segregation.

Method

Participants – HCP

Preprocessed resting-state functional MRI (rsfMRI) data from the S1200 Release of Human Connectome Project (WU-UMN HCP Consortium) were downloaded for analysis. Only data for unrelated, right-handed (Handedness>24) individuals without psychiatric diagnoses were used. Data were considered for this study only if the participant attained a high school degree (SSAGA_Educ>11), reported no family history of mental illness (FamHist_*_None = 1), did not meet the DSM4 criteria for Alcohol Abuse or Dependence (SSAGA_Alc_D4_Ab_Dx != 5; SSAGA_Alc_D4_Dp_Dx != 5), and did not meet the DSM criteria for Marijuana Dependence (SSAGA_Mj_Ab_Dep = 0). To account for any potential familial similarities in brain structure and function, only one participant from each family unit was chosen. Using Excel's Rand() function, each participant was assigned a random number and the participant with the largest number in their family was selected for inclusion in the analyses. Only participants with a complete set of data (one T1w structural and four resting-state fMRI sessions with the associated movement parameters) were used for analysis. These exclusions resulted in a sample size of 233 individuals ranging in age from 22 to 37 years (111 males, 122 females; see Supplemental Text 1). Detailed descriptions of each variable used to eliminate participants are available here: https://wiki.humanconnectome.org (see HCP Data Dictionary Public- Updated for the 1200 Subject Release).

HCP image acquisition and preprocessing

rsfMRI data for each participant consisted of four 15-minute runs collected over 2 sessions on different days (1200 volumes, 720 ms TR, 2 mm isotropic voxels; see Van Essen et al. (2012) for full details on fMRI acquisition). Notably, there were no differences in functional connectivity

between the two sessions (see Supplemental Text 2 for detailed analysis methods and results). Preprocessed T1w structural, functional, and motion regressor data were downloaded from the HCP S1200 Release Amazon Web Services repository. Details of the preprocessing pipeline for functional images are fully described in Glasser et al. (2013). Structural scans had undergone gradient distortion correction, bias field correction, and registration to the 0.8 mm resolution MNI brain using Multimodal Surface Matching (Glasser et al., 2013, 2016). Additionally, structural images underwent tissue type segmentation and functional images underwent smoothing (5 mm FWHM) and artifact detection (global signal z-value threshold: 5, subject motion threshold: 0.9 mm) using the CONN toolbox (v. 20b; Whitfield-Gabrieli & Nieto-Castanon, 2012), a Matlab-based application designed for functional connectivity analysis and MATALB R2019b on centOS 7. Functional data were then denoised using confound regressors for 5 temporal components each from the segmented CSF and white matter, 24 motion realignment parameters, signal and/or motion outliers, and the 1st order derivative from the effect of rest. Finally, data underwent linear detrending and bandpass filtering (0.008 - 0.09 Hz).

Regions of interest

Using fslmaths, 3.5 mm spherical, binarized regions of interest (ROIs) representing two rsfMRI networks of CB and BG nodes (cognitive and motor CB-BG network), and 7 rsfMRI cortical networks (3 cognitive-associated, FPN, CON, DMN; 1 motor-associated, MN; 1 emotion-associated, EN; and two sensory-associated, VN, AN) were created with coordinates from previous works (FSL v.6.0.3: FMRIB's Software Library, www.fmrib.ox.ac.uk/fsl; Jenkinson, Beckmann, Behrens, Woolrich, & Smith, 2012). CB-BG network ROIs were created using CB and BG coordinates previously used in our recent work (Hausman et al., 2019). Lob V and Lob VI of the CB and dorsal caudal and dorsal rostral putamen of the BG were used to define the MCBN; while,

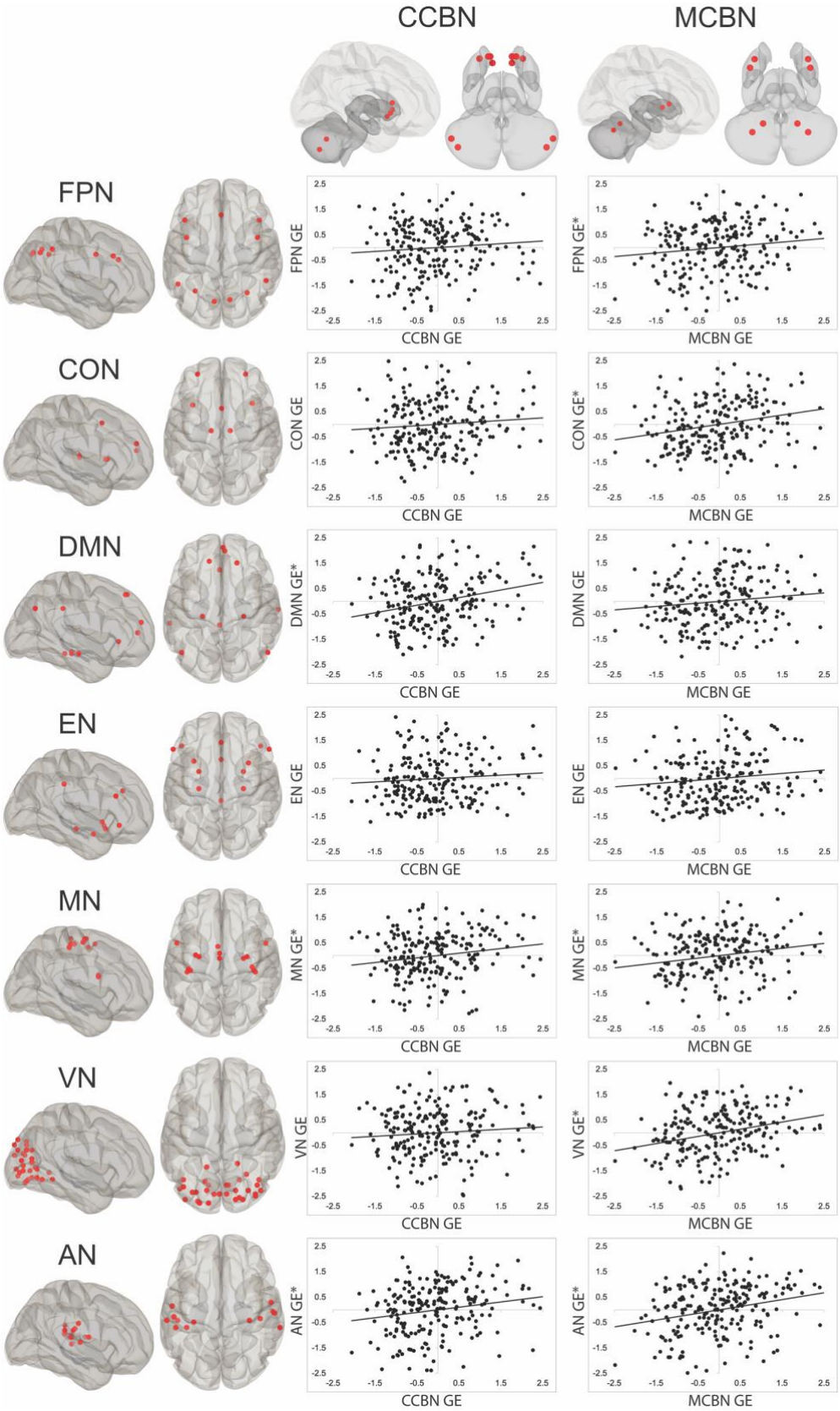

Figure 1. ROI locations for each network and scatterplots depicting the relationship between CCBM or MCBN GE and cortical network GE. To represent the partial correlations conducted in the analysis, standardized residuals of each CB-BG network (each controlling for the other) and standardized residuals of each cortical measure (controlling for the CB-BG network not in the analysis) were used. *Statistically significant correlation.

Crus I and Crus II of the CB and the inferior and superior ventral striatum, dorsal caudate, and

ventral rostral putamen of the BG were used to define the CCBN. This division is in line with previous work parcellating each region based on resting-state and task-based functional connectivity and behavioral associations (Bernard et al., 2012; Di Martino et al., 2008; Salmi et al., 2010; Stoodley et al., 2012)

The cognitive networks were defined using ROIs from two task-positive rsfMRI networks, the cingulo-opercular (CON) and the fronto-parietal (FPN), and the default mode network (DMN), using coordinates originally reported by Fair et al. (2009). Motor network (MN) ROIs were created using coordinates based on Mayka, Corcos, Leurgans, & Vaillancourt (2006). Emotional Network (EN) ROIs were created using coordinates originally reported by Stein et al. (2007) and adapted using information from Deen, Pitskel, & Pelphrey, (2011). The visual and auditory sensory networks, VN and AN, were defined using coordinates reported by Cassady et al. (2019). Importantly, given the association the CB and BG have with cortical and limbic networks, especially the MN, we did not use any CB or BG ROIs in any of the cortical networks. This required change of the VN only, for which we removed an ROI for CB Lobule VI. Removing this ROI allowed us to directly correlate measures from within the CB-BG networks to measures from within cortical networks. To account for the use of both left and right ROIs in some cortical networks, all lateralized (defined as more than 3mm from the midline in the x direction) ROIs without a reported contralateral match were mirrored inthe x direction (see Supplemental Table 2 for parallel analysis using only the original ROIs). Supplemental Table 1 and Figure 1 provide details for the 122 resulting ROIs. ROIs will be referred to by their abbreviation in Table 1 from this point forward.

fMRI participant-level correlation matrices

For each participant, a timeseries for each of the 122 ROIs was extracted and cross-correlated using bivariate analyses, resulting in a correlation matrix for each participant. All participant-level analyses were performed in the CONN toolbox (v. 20b; Whitfield-Gabrieli & Nieto-Castanon, 2012).

Subcortical network analysis – replication

Subcortical ROIs originally used in our recent investigation of CB-BG connectivity in young and older adults (Hausman et al. 2019) were used to replicate the findings in a larger sample, again computed using the CONN toolbox (v. 20b; Whitfield-Gabrieli & Nieto-Castanon, 2012). Bivariate correlations were calculated by cross correlating each timeseries of four lateralized CB ROIs (R CrusI, R CrusII, R LobV, and R LobVI) and six lateralized BG ROIs (L VSi, L VSs, L VRP, L DRP, L DC, L DCP). Fisher z-transformed correlation matrices were computed and thresholded at p(FDR) = .05.

Graph theory and correlational analyses

Average network-level graph theoretical measures were computed separately for each of the seven networks within the CONN toolbox (Whitfield-Gabrieli & Nieto-Castanon, 2012). Edges were defined as thresholded positive correlation coefficients ($\beta > .1$) and nodes were defined as the ROIs in a given network (Fair et al., 2009). Given previous findings that show a high degree of integration within each network (Fair et al., 2009; Geerligs et al., 2015; Hausman et al., 2019; Stein et al., 2007), we focused on network-level GE, a measure of how efficiently information in a network travels, as the primary measure of each network's integration for our analyses here (Achard & Bullmore, 2007; Latora & Marchiori, 2001; Sheffield et al., 2016; Whitfield-Gabrieli & Nieto-Castanon, 2012). To test whether the GE of the CB-BG networks were related to the GE of the FPN, CON, DMN, EN, MN, VN, or AN, partial Pearson correlations were performed

between the each of the CB-BG networks and each of the other networks (i.e., CCBN GE compared to FPN GE) using IBM SPSS 25 (IBM Corporation Armonk, NY, 2017). We also calculated the following network-level graph theoretical measures and performed the same analyses in order to compare the findings in an exploratory manner: betweenness centrality (average of the number of times each node is part of a shortest-path between any two ROIs), cost/degree (average of the proportion/number of edges that are connected to a given node - for our purposes, cost and degree are redundant measures and are discussed as one), and average path length (average number of edges traversed from ROI-to-ROI). For a full mathematical description of each of these measures and of GE, please see Achard & Bullmore, 2007; Latora & Marchiori, 2001; Rubinov & Sporns, 2010; Sporns et al., 2004 and Whitfield-Gabrieli & Nieto-Castanon, 2012. Bonferroni corrections were applied to all exploratory correlations.

Network segregation analysis

Participant-level Fisher z-transformed correlation matrices were used to calculate within-network and between-network connectivity separately for each network (Chan et al., 2014). Within-network connectivity was defined as the average z-score for all ROI-to-ROI connections in a network. Between-network connectivity was defined differently for the CB-BG and cortical networks. For each of the CB-BG networks, between-network connectivity was defined as the average z-score of the ROI-to-ROI connections between nodes in the CCBN and nodes in the MCBN. For all cortical networks, between-network connectivity was defined as the average z-score of the ROI-to-ROI connections between all nodes in every other cortical network (leaving out all CB-BG nodes). This allowed us to test whether motor and cognitive node segregation within the CB and BG (and vice versa) was related to the segregation of cortical networks. Next, network segregation was calculated separately for each network using the following formula:

$$\frac{Zwithin - Zbetween}{Zwithin}$$

To answer the question of whether subcortical segregation predicted cortical segregation, Pearson correlations were performed between the CB-BG networks and each cortical network's segregation score. We chose to use bivariate, as opposed to partial, correlations for the segregation analyses, due to the nature of how both CB-BG networks are measured when segregation is calculated.

Results

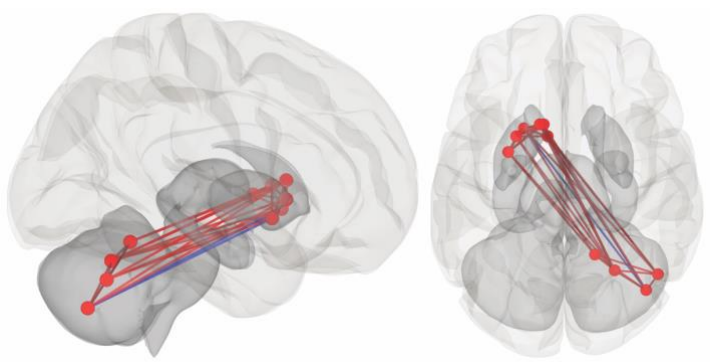

Figure 2. Right and superior views of connectivity patterns within right CB and left BG seeds.

CB-BG connectivity network

Figure 2 depicts the connectivity patterns and Table 1 lists *t*-scores and beta values for each ROI-to-ROI pair in the lateralized CB-BG network analysis, performed to replicate our previous findings in a larger sample (Hausman et al., 2019). Broadly speaking,

Table 1. β values and paired *t*-tests and for each significant ROI-ROI pair.

ROI pairs	β	*t* (222)	*p* (FDR)
R CrusI - R CrusII	0.07	12.89	0.001
R CrusI - R LobV	0.01	2.88	.008
R CrusI -R LobVI	0.02	5.09	0.001
R CrusI - L VSi	0.01	2.8	.008
R CrusI - L VRP	0.02	6.16	0.001
R CrusI - L DC	0.02	5.83	0.001
R CrusII - R LobV	0.01	2.94	.006
R CrusII - R LobVI	0.01	4.21	0.001
R CrusII - L VSs	0.01	3	.006
R CrusII - L VSi	-0.01	-2.2	.04
R CrusII - L VRP	-0.01	-2.84	.007
R CrusII - L DC	0.01	3.97	0.001
R LobV - R LobVI	0.02	7.15	0.001
R LobV - L DRP	0.01	3.35	0.003
R LobV - L DCP	0.02	5.69	0.001
R LobVI - L VSs	0.01	2.38	.02
R LobVI - L VSi	0.01	2.23	.03
R LobVI - L VRP	0.01	3.01	.004
R LobVI - L DRP	0.02	5.32	0.001
R LobVI - L DCP	0.01	4.23	0.001
R LobVI - L DC	0.02	4.54	0.001
L VRP - L VSs	0.07	16.93	0.001
L VRP - L VSi	0.04	12.7	0.001
L VRP - L DC	0.07	18.02	0.001
L DRP - L VSs	0.03	7.95	0.001
L DRP - L VSi	0.01	4.18	0.001
L DRP - L VRP	0.11	24.52	0.001
L DRP - L DC	0.05	13.83	0.001
L DCP - L VSs	0.01	3.44	0.001
L DCP - L VRP	0.06	15.84	0.001
L DCP - L DRP	0.12	26.71	0.001
L DCP - L DC	0.03	8.07	0.001
L DC - L VSs	0.05	12.17	0.001
L DC - L VSi	0.02	7.47	0.001
L VSi - L VSs	0.03	10.01	0.001

these results successfully replicate our past work showing robust positive connectivity between the CB and BG. Notably, these analyses did reveal 2 anticorrelations that were not seen in our prior work (Hausman et al., 2019). These anticorrelations were seen between R CrusII and both L VSi and L VRP. We suspect however, that the anticorrelations found here may be due to higher sensitivity and statistical power associated with the larger sample used in this investigation.

Subcortical-cortical graph theory network-level correlations

Table 2. Pearson correlation values (*r's)* for each subcortical-cortical pairing.

	FPN	CON	DMN	EN	MN	VN	AN
CCBN GE	**.10**	**.10**	**.30*** **	**.09**	**.18** **	**.09**	**.21** **
MCBN GE	**.14* **	**.25** **	**.13**	**.13**	**.19** **	**.28*** **	**.27*** **
CCBN Seg	**.00**	**-.02**	**-.01**	**.00**	**-.02**	**-.03**	**.01**
MCBN Seg	**-.02**	**.02**	**-.03**	**.00**	**.19** **	**.04**	**.03**
CCBN BC	-.04	.03	.24***	.06	-.08	-.11	-.02
MCBN BC	-.11	.19**	.05	.08	-.10	-.14	.04
CCBN C/D	.13	.12	.23***	.12	.15*	.06	.23***
MCBN C/D	.19**	.22**	.17*	.16*	.25***	.29***	.26***
CCBN APL	-.06	.03	.12	.08	-.14	-.10	-.11
MCBN APL	-.13	.14	.02	.01	-.04	-.10	-.04

Note. Main analyses (bolded) were assessed for significance at p < .05. Exploratory analyses were assessed using an FDR correction. ***p < .001 **p < .01 *p < .05.
Abbreviations: Cognitive Cerebellum-Basal Ganglia Network (CCBN); Motor Cerebellum-Basal Ganglia Network (MCBN); Global Efficiency (GE); Segregation (Seg); Betweenness Centrality (BC); Cost and Degree (C/D); Average Path Length (APL)

Table 2 lists partial Pearson correlation coefficients (r) and Figure 1 depicts the scatterplots for relationships between CB-BG and cortical network GE. A positive correlation was found between CCBN GE and DMN GE, in line with our predictions. We additionally found unexpected positive correlations between the GE of CCBN and that of MN and AN. No associations between CCBN GE and FPN and CON GE were found, contrary to our hypotheses. MCBN network GE positively correlated with the MN, VN, and AN, as predicted. Positive correlations were also found between MCBN GE and FPN and CON GE, unexpectedly. There

were no associations between MCBN GE and EN GE. For a complete picture of cortical network integration, exploratory correlational analyses between cortical and limbic network GE are presented in Supplemental Table 3. Positive correlations were found between every network pairing except for FPN/EN.

Table 2 lists partial Pearson correlation coefficients (r) for relationships between CB-BG and cortical network segregation. CCBN segregation did not correlate with any cortical network segregation, contrary to our hypotheses. MCBN segregation correlated with MN, in line with our hypotheses. No other correlations involving segregation were found ($ps > .06$). We also explored correlations between cortical network segregation. We found significant positive correlations between CON and VN segregation ($r(221) = .21$, $p = .01$), and between MN and both sensory networks (VN, $r(221) = .39$, $p < .001$; AN, $r(221) = .33$, $p < .001$). We also found a significant negative correlation between FPN and AN segregation ($r(221) = -.15$, $p = .04$). No other significant correlations were found between any cortical network ($ps > .07$).

The exploratory correlations between CB-BG and cortical/limbic graph theory measures are also presented in Table 2. Cost and degree of the CCBN correlated with that of the DMN, MN, and AN, in line with the GE results. Cost and degree of the MCBN correlated with that of FPN, CON, MN, VN, and AN, mirroring the GE analyses, and additionally the DMN and EN. Betweenness centrality (BC) of the CCBN positively correlated with that of the DMN. MCBN network BC positively correlated with that of the CON. No other subcortical-cortical correlations were found when using betweenness centrality. No correlations were found using APL as a network metric.

Discussion

Here, we performed novel correlational analyses relating cognitive and motor CB-BG network GE to cortical network GE to investigate whether the integration and separation of CB-BG networks correlates with that of cortical networks, as would be predicted given Bostan & Strick's (2018) hypothesis that the CB-BG network is foundational to cortical networks and cognition. These results suggest some degree of specificity of cognitive/motor CB-BG networks as they relate to cortical networks. This has implications for understanding cortical network processing and cortical-subcortical interactions in healthy adults and may help in understanding the broad network-based changes seen in disease states.

First, we replicated our previous work (Hausman et al., 2019) investigating CB-BG connectivity at rest and report strong connectivity between these subcortical regions. Our findings are consistent with our prior work demonstrating robust connectivity between the CB and the BG, but this replication revealed several new findings as well. Within the CB, we found associations between every lateralized node, and a similar pattern again emerged within the BG. We also found that R LobVI is functionally connected to every BG ROI, reflecting R LobVI's role in both motor and cognitive function (Balsters et al., 2013) and the functional connections to premotor, motor, and prefrontal area (Bernard et al., 2012). However, we also found anticorrelations for R CrusII - L VSi and R CrusII - L VRP connections. This may be indicative of delayed or lagged communication between these regions but the best interpretation of negative relationships between time courses is up for debate (Meszlényi et al., 2017).

Contrary to our predictions about task-positive cognitive networks, we found that FPN and CON GE were significantly related to the MCBN GE, yet we found only marginal associations between CCBN GE and FPN and CON GE. The relationship between FPN and MCBN integration may be due to the involvement of CB Lob VI in cognition and working memory, cognitive control,

and response inhibition (Balsters et al., 2013; Bernard et al., 2020; Clark et al., 2020; Von der Gablentz et al., 2015), while the relationship with CON integration is perhaps due to the network's association with alertness and error processing (Coste & Kleinschmidt, 2016; Neta et al., 2014). Regarding cognitive networks, it may be that efficiency within motor nodes of the CB-BG network may be more related to cognition than efficiency within the cognitive nodes; however, while there is a difference between the CB-BG networks in their relationships with the FPN, the effect sizes are similar (*rs* = .10 and .14), so caution must be taken in interpreting the differences.

In line with our predictions, the GE of the DMN, a task-negative network associated with self-reflective thought and mind-wandering (Fox et al., 2015), was related to CCBN GE, highlighting the role of the CB and BG in this key network. However, DMN segregation from cortical networks was not related to segregation of CCBN from the MCBN network, inconsistent with our predictions. It seems that while the integration of cognitive regions of the CB-BG network may support DMN processing, separation of CB-BG cognitive regions from motor systems is not related to DMN function in healthy adults.

The GE of both CB-BG networks correlated positively with MN GE, indicating that the CB and BG are involved not only with motor behavior, through its association with the MN (Bernard et al., 2014; Jackson et al., 2020; Kelly & Strick, 2003, 2004), but also with cognitive control via the prefrontal-cortical loops that innervate the CCBN (Bostan & Strick, 2018; Da Cunha et al., 2012; Haber, 2014; Schmidt et al., 2008; Sgambato-Faure et al., 2016; Yin et al., 2008). Additionally, MCBN segregation correlated positively with MN segregation, highlighting the importance of motor segregation in healthy young adults.

Sensory network GE positively correlated with MCBN GE, as expected due to previous functional parcellations of the CB and BG (Buckner et al., 2011; Di Martino et al., 2008) and their

historical associations with motor behavior. Interestingly, CCBN GE also correlated with AN GE, possibly due to subvocalization and auditory loops used in cognition and verbal working memory (Rottschy et al., 2012). MCBN segregation correlated with AN segregation, indicating that, while CCBN integration may be important for subvocalization, the separation of motor from cognitive regions of the CB-BG network is important for sound and language processing, potentially due to CB-BG involvement in discriminating between subvocal cognition and sensory stimuli processing, as is thought to break down in psychosis-related disorders (e.g., Debbané et al., 2010).

No relationships were found between either the CCBN or MCBN and the EN. We originally predicted that due to the involvement of Lobule VI in emotional processes (Riedel et al., 2015), that MCBN GE and segregation would correlate positively with that of the EN. However, our null results indicate that efficiency and segregation of the cognitive and motor CB-BG networks is not related to the EN. We think this may be in part due to the method by which limbic regions within the EN communicate with the cortex. The amygdala and related structures project to cortical regions directly (MacLean, 1988), indicating limbic regions may have evolved to support cortical behavior independent of CB-BG interactions, perhaps to decrease the time it takes to relay important information like the identification of a threat.

To further understand the relationships between the CB-BG network and cortical networks, parallel exploratory analyses were conducted using other graph theory measures. Cost and degree analyses generally replicated the main GE analyses (see Table 2). This was expected, as these are measures of the number of connections in a network and are proxies for network efficiency (Rubinov & Sporns, 2010). BC, a measure of the average proportion of times that an ROI in a network is part of the shortest ROI-to-ROI path within the network (Rubinov & Sporns, 2010), showed a relationship between the CCBN and the DMN, in line with GE analyses. MCBN BC

correlated with the CON and VN BC, highlighting motor involvement with alertness and attention (Coste & Kleinschmidt, 2016; Neta et al., 2014), partially mirroring the GE analyses. Similarly, APL only related the MCBN with the CON and VN, indicating that BC and APL are potentially not as sensitive as cost and degree or GE in determining relationships between subcortical-cortical pairs. This may be because not all within-network ROIs are connected, resulting in ROIs with zero efficiency being left out of the equations for C/D, APL, and BC and thus failing to fully capture the efficiency of the network. GE solves this issue by including ROI connections that have zero efficiency (Rubinov & Sporns, 2010), and provides further support for using GE in our analyses. Together, these exploratory findings help to confirm the idea that subcortical integration is related to the integration of large-scale cortical networks, though the degree to which this is the case varies by integration measure.

Limitations

While this work provides important new insights into the interplay between subcortical CB-BG networks and those in the cortex, there are several limitations to consider. For each network, we used an unequal number of ROIs that represent a subset of the possible ROIs that could be used to investigate these networks. These choices were rooted in the literature of canonical resting-state networks (Deen et al., 2011; Fair et al., 2009; Mayka et al., 2006; Stein et al., 2007) but accounting for the disparate number of regions, using a whole-brain parcellation approach, or defining ROIs within a network using a more data-driven method may produce different results and these methods warrant their own studies. Future studies may also benefit from simply increasing the number of ROIs, allowing for higher resolution when capturing network measures. CB-BG networks may generally benefit from adding ROIs that incorporate additional areas within each region (i.e. including additional domain-associated CB nodes in each network; including BG

regions other than the striatum, caudate, and putamen). In particular, a meta-analysis detailed emotional processing withing CB Lobules IV, V, VI, VIII, and IX (E et al., 2014) and perhaps a relationship with the EN would be found using different nodes or an additional CB-BG network. Relatedly, there are additional cortical networks that can be included. For example, we examined the CON network but did not distinguish between the ventral and dorsal attention systems. Additional ROIs and networks may help better capture information travel and integration and assist in deciphering complicated cortical-CB-BG relationships.

Additionally, although there are CB and BG nodes known to be involved in many of the cortical resting-state networks, the cortical networks chosen for use did not include any CB or BG ROIs (a single CB node within the VN was removed prior to analyses). This allowed us to directly compare CB-BG and cortical network patterns. While necessary for our purposes, this method inherently truncates the size of the functional networks to only cortical nodes, potentially limiting the accuracy of the network measure in the context of how these networks are recruited during task processing. Lastly, we used classic time-series autocorrelational analyses to build an ROI-to-ROI table. Other methods that can account for temporal lag like dynamic time warping (Meszlényi 2017) or sliding window analyses may reveal additional details about the temporal order of activation in within-network ROI relationships that are used to calculate the graph theory measures.

Conclusions

These findings suggest CB-BG network integration is related to cortical network integration, and cognitive/motor segregation is important for cortical processing, in support of theories suggesting that the CB and BG each serve a foundational role for learning and cognition in support of domain-specific cortical networks (Bostan & Strick, 2018). We also showed that,

while regions associated with similar behavioral domains (cognitive, motor, etc.) tend to be highly functionally connected (Bernard et al., 2013; Hausman et al., 2019), CB and BG subregions are generally highly functionally connected, even between regions associated with different behavioral domains and cortical circuitsExploring the CB-BG relationship and their cortical projections within the context of psychopathologies would be interesting and worthwhile. These findings detail network dynamics in a large representative sample and may help to elucidate network-related changes in clinical or older adult populations in the future.

References

Achard, S., & Bullmore, E. (2007). Efficiency and Cost of Economical Brain Functional Networks. *PLoS Computational Biology*, *3*(2), e17. https://doi.org/10.1371/journal.pcbi.0030017

Anticevic, A., Cole, M. W., Repovs, G., Murray, J. D., Brumbaugh, M. S., Winkler, A. M., Savic, A., Krystal, J. H., Pearlson, G. D., & Glahn, D. C. (2014). Characterizing Thalamo-Cortical Disturbances in Schizophrenia and Bipolar Illness. *Cerebral Cortex*, *24*(12), 3116–3130. https://doi.org/10.1093/cercor/bht165

Argyelan, M., Carbon, M., Niethammer, M., Ulug, A. M., Voss, H. U., Bressman, S. B., Dhawan, V., & Eidelberg, D. (2009). Cerebellothalamocortical Connectivity Regulates Penetrance in Dystonia. *Journal of Neuroscience*, *29*(31), 9740–9747. https://doi.org/10.1523/JNEUROSCI.2300-09.2009

Argyropoulos, G. P. D., van Dun, K., Adamaszek, M., Leggio, M., Manto, M., Masciullo, M., Molinari, M., Stoodley, C. J., Van Overwalle, F., Ivry, R. B., & Schmahmann, J. D. (2020). The Cerebellar Cognitive Affective/Schmahmann Syndrome: a Task Force Paper. *Cerebellum*, *19*(1), 102–125. https://doi.org/10.1007/s12311-019-01068-8

Asanuma, K. (2006). Network modulation in the treatment of Parkinson's disease. *Brain*, *129*(10), 2667–2678. https://doi.org/10.1093/brain/awl162

Balsters, J. H., Cussans, E., Diedrichsen, J., Phillips, K. A., Preuss, T. M., Rilling, J. K., & Ranganath, C. (2010). Evolution of the cerebellar cortex: The selective expansion of prefrontal-projecting cerebellar lobules. *NeuroImage*, *49*(3), 2045–2052. https://doi.org/10.1016/j.neuroimage.2009.10.045

Balsters, J. H., & Ranganath, C. (2008). Symbolic representations of action in the human

cerebellum. *NeuroImage*, *43*(2), 388–398. https://doi.org/10.1016/j.neuroimage.2008.07.010

Balsters, J. H., Whelan, C. D., Robertson, I. H., & Ramnani, N. (2013). Cerebellum and cognition: Evidence for the encoding of higher order rules. *Cerebral Cortex*, *23*(6), 1433–1443. https://doi.org/10.1093/cercor/bhs127

Barton, R. A., & Venditti, C. (2014). Rapid Evolution of the Cerebellum in Humans and Other Great Apes. *Current Biology*, *24*(20), 2440–2444. https://doi.org/10.1016/j.cub.2014.08.056

Bell, C. C. (2002). *Evolution of Cerebellum-Like Structures*. *2002*, 312–326.

Bernard, J. A., Nguyen, A. D., Hausman, H. K., Maldonado, T., Ballard, H. K., Jackson, T. B., Eakin, S. M., Lokshina, Y., & Goen, J. R. M. (2020). Shaky scaffolding: Age differences in cerebellar activation revealed through activation likelihood estimation meta-analysis. *Human Brain Mapping*, *41*(18), 5255–5281. https://doi.org/10.1002/hbm.25191

Bernard, J. A., Peltier, S. J., Benson, B. L., Wiggins, J. L., Jaeggi, S. M., Buschkuehl, M., Jonides, J., Monk, C. S., & Seidler, R. D. (2014). Dissociable Functional Networks of the Human Dentate Nucleus. *Cerebral Cortex*, *24*(8), 2151–2159. https://doi.org/10.1093/cercor/bht065

Bernard, J. A., Peltier, S. J., Wiggins, J. L., Jaeggi, S. M., Buschkuehl, M., Fling, B. W., Kwak, Y., Jonides, J., Monk, C. S., & Seidler, R. D. (2013). Disrupted cortico-cerebellar connectivity in older adults. *NeuroImage*, *83*, 103–119. https://doi.org/10.1016/j.neuroimage.2013.06.042

Bernard, J. A., Seidler, R. D., Hassevoort, K. M., Benson, B. L., Welsh, R. C., Wiggins, J. L., Jaeggi, S. M., Buschkuehl, M., Monk, C. S., Jonides, J., & Peltier, S. J. (2012). Resting state cortico-cerebellar functional connectivity networks: a comparison of anatomical and self-

organizing map approaches. *Frontiers in Neuroanatomy*, *6*(August), 1–19. https://doi.org/10.3389/fnana.2012.00031

Bo, J., Lee, C.-M., Kwak, Y., Peltier, S. J., Bernard, J. A., Buschkuehl, M., Jaeggi, S. M., Wiggins, J. L., Jonides, J., Monk, C. S., & Seidler, R. D. (2014). Lifespan Differences in Cortico-Striatal Resting State Connectivity. *Brain Connectivity*, *4*(3), 166–180. https://doi.org/10.1089/brain.2013.0155

Bostan, A. C., Dum, R. P., & Strick, P. L. (2010). The basal ganglia communicate with the cerebellum. *Proceedings of the National Academy of Sciences*, *107*(18), 8452–8456. https://doi.org/10.1073/pnas.1000496107

Bostan, A. C., & Strick, P. L. (2018). The basal ganglia and the cerebellum: Nodes in an integrated network. *Nature Reviews Neuroscience*, *19*(6), 338–350. https://doi.org/10.1038/s41583-018-0002-7

Buckner, R. L., Andrews-Hanna, J. R., & Schacter, D. L. (2008). The Brain's Default Network. *Annals of the New York Academy of Sciences*, *1124*(1), 1–38. https://doi.org/10.1196/annals.1440.011

Buckner, R. L., Krienen, F. M., Castellanos, A., Diaz, J. C., & Yeo, B. T. T. (2011). The organization of the human cerebellum estimated by intrinsic functional connectivity. *Journal of Neurophysiology*, *106*(5), 2322–2345. https://doi.org/10.1152/jn.00339.2011

Caligiore, D., Helmich, R. C., Hallett, M., Moustafa, A. A., Timmermann, L., Toni, I., & Baldassarre, G. (2016). Parkinson's disease as a system-level disorder. *Nature Publishing Group Parkinson's Disease*, *2*(1), 16025. https://doi.org/10.1038/npjparkd.2016.25

Cassady, K., Gagnon, H., Lalwani, P., Simmonite, M., Foerster, B., Park, D. C., Peltier, S. J., Petrou, M., Taylor, S. F., Weissman, D. H., Seidler, R. D., & Polk, T. A. (2019).

NeuroImage Sensorimotor network segregation declines with age and is linked to GABA and to sensorimotor performance. *NeuroImage*, *186*(July 2018), 234–244. https://doi.org/10.1016/j.neuroimage.2018.11.008

Chan, M. Y., Park, D. C., Savalia, N. K., Petersen, S. E., & Wig, G. S. (2014). Decreased segregation of brain systems across the healthy adult lifespan. *Proceedings of the National Academy of Sciences*, *111*(46), E4997–E5006. https://doi.org/10.1073/pnas.1415122111

Chen, S. H. A., & Desmond, J. E. (2005). Temporal dynamics of cerebro-cerebellar network recruitment during a cognitive task. *Neuropsychologia*, *43*(9), 1227–1237. https://doi.org/10.1016/j.neuropsychologia.2004.12.015

Clark, S. V., King, T. Z., & Turner, J. A. (2020). Cerebellar Contributions to Proactive and Reactive Control in the Stop Signal Task: A Systematic Review and Meta-Analysis of Functional Magnetic Resonance Imaging Studies. *Neuropsychology Review*, *30*(3), 362–385. https://doi.org/10.1007/s11065-020-09432-w

Coste, C. P., & Kleinschmidt, A. (2016). Cingulo-opercular network activity maintains alertness. *NeuroImage*, *128*, 264–272. https://doi.org/10.1016/j.neuroimage.2016.01.026

Da Cunha, C., Gomez-A, A., & Blaha, C. D. (2012). The role of the basal ganglia in motivated behavior. *Reviews in the Neurosciences*, *23*(5–6), 747–767. https://doi.org/10.1515/revneuro-2012-0063

Debbané, M., Van Der Linden, M., Glaser, B., & Eliez, S. (2010). Monitoring of self-generated speech in adolescents with 22q11.2 deletion syndrome. *British Journal of Clinical Psychology*, *49*(3), 373–386. https://doi.org/10.1348/014466509X468223

Deen, B., Pitskel, N. B., & Pelphrey, K. A. (2011). Three Systems of Insular Functional Connectivity Identified with Cluster Analysis. *Cerebral Cortex*, *21*(7), 1498–1506.

https://doi.org/10.1093/cercor/bhq186

DeLong, M., & Wichmann, T. (2010). Changing Views of Basal Ganglia Circuits and Circuit Disorders. *Clinical EEG and Neuroscience*, *41*(2), 61–67. https://doi.org/10.1177/155005941004100204

Di Martino, A., Scheres, A., Margulies, D. S., Kelly, A. M. C., Uddin, L. Q., Shehzad, Z., Biswal, B., Walters, J. R., Castellanos, F. X., & Milham, M. P. (2008). Functional Connectivity of Human Striatum: A Resting State fMRI Study. *Cerebral Cortex*, *18*(12), 2735–2747. https://doi.org/10.1093/cercor/bhn041

Draganski, B., Kherif, F., Kloppel, S., Cook, P. A., Alexander, D. C., Parker, G. J. M., Deichmann, R., Ashburner, J., & Frackowiak, R. S. J. (2008). Evidence for Segregated and Integrative Connectivity Patterns in the Human Basal Ganglia. *Journal of Neuroscience*, *28*(28), 7143–7152. https://doi.org/10.1523/JNEUROSCI.1486-08.2008

E, K.-H., Chen, S.-H. A., Ho, M.-H. R., & Desmond, J. E. (2014). A meta-analysis of cerebellar contributions to higher cognition from PET and fMRI studies. *Human Brain Mapping*, *35*(2), 593–615. https://doi.org/10.1002/hbm.22194

Fair, D. A., Cohen, A. L., Power, J. D., Dosenbach, N. U. F., Church, J. A., Miezin, F. M., Schlaggar, B. L., & Petersen, S. E. (2009). Functional Brain Networks Develop from a "Local to Distributed" Organization. *PLoS Computational Biology*, *5*(5), e1000381. https://doi.org/10.1371/journal.pcbi.1000381

Fox, K. C. R., Spreng, R. N., Ellamil, M., Andrews-Hanna, J. R., & Christoff, K. (2015). The wandering brain: Meta-analysis of functional neuroimaging studies of mind-wandering and related spontaneous thought processes. *NeuroImage*, *111*, 611–621. https://doi.org/10.1016/j.neuroimage.2015.02.039

Geerligs, L., Renken, R. J., Saliasi, E., Maurits, N. M., & Lorist, M. M. (2015). A Brain-Wide Study of Age-Related Changes in Functional Connectivity. *Cerebral Cortex*, *25*(7), 1987–1999. https://doi.org/10.1093/cercor/bhu012

Glasser, M. F., Smith, S. M., Marcus, D. S., Andersson, J. L. R., Auerbach, E. J., Behrens, T. E. J., Coalson, T. S., Harms, M. P., Jenkinson, M., Moeller, S., Robinson, E. C., Sotiropoulos, S. N., Xu, J., Yacoub, E., Ugurbil, K., & Van Essen, D. C. (2016). The Human Connectome Project's neuroimaging approach. *Nature Neuroscience*, *19*(9), 1175–1187. https://doi.org/10.1038/nn.4361

Glasser, M. F., Sotiropoulos, S. N., Wilson, J. A., Coalson, T. S., Fischl, B., Andersson, J. L., Xu, J., Jbabdi, S., Webster, M., Polimeni, J. R., Van Essen, D. C., & Jenkinson, M. (2013). The minimal preprocessing pipelines for the Human Connectome Project. *NeuroImage*, *80*, 105–124. https://doi.org/10.1016/j.neuroimage.2013.04.127

Griffanti, L., Stratmann, P., Rolinski, M., Filippini, N., Zsoldos, E., Mahmood, A., Zamboni, G., Douaud, G., Klein, J. C., Kivimäki, M., Singh-Manoux, A., Hu, M. T., Ebmeier, K. P., & Mackay, C. E. (2018). Exploring variability in basal ganglia connectivity with functional MRI in healthy aging. *Brain Imaging and Behavior*, *12*(6), 1822–1827. https://doi.org/10.1007/s11682-018-9824-1

Grillner, S., & Robertson, B. (2016). The Basal Ganglia Over 500 Million Years. *Current Biology*, *26*(20), R1088–R1100. https://doi.org/10.1016/j.cub.2016.06.041

Guell, X., Gabrieli, J. D. E., & Schmahmann, J. D. (2018). Triple representation of language, working memory, social and emotion processing in the cerebellum: convergent evidence from task and seed-based resting-state fMRI analyses in a single large cohort. *NeuroImage*, *172*(January), 437–449. https://doi.org/10.1016/j.neuroimage.2018.01.082

Haber, S. N. (2014). The place of dopamine in the cortico-basal ganglia circuit. *Neuroscience*, *282*(12), 248–257. https://doi.org/10.1016/j.neuroscience.2014.10.008

Hausman, H. K., Jackson, T. B., Goen, J. R. M., & Bernard, J. A. (2019). From Synchrony to Asynchrony: Cerebellar–Basal Ganglia Functional Circuits in Young and Older Adults. *Cerebral Cortex*, *41*(18), 5255–5281. https://doi.org/10.1093/cercor/bhz121

Herrick M.D., C. J. (1924). Origin and Evolution of the Cerebellum. *Archives of Neurology and Psychiatry*, *11*(6), 621–652.

Hoshi, E., Tremblay, L., Féger, J., Carras, P. L., & Strick, P. L. (2005). The cerebellum communicates with the basal ganglia. *Nature Neuroscience*, *8*(11), 1491–1493. https://doi.org/10.1038/nn1544

Jackson, T. B., Maldonado, T., Eakin, S. M., Orr, J. M., & Bernard, J. A. (2020). Cerebellar and prefrontal-cortical engagement during higher-order rule learning in older adulthood. *Neuropsychologia*, *148*(July), 107620. https://doi.org/10.1016/j.neuropsychologia.2020.107620

Jenkinson, M., Beckmann, C. F., Behrens, T. E. J., Woolrich, M. W., & Smith, S. M. (2012). FSL. *NeuroImage*, *62*(2), 782–790. https://doi.org/10.1016/j.neuroimage.2011.09.015

Ji, J. L., Diehl, C., Schleifer, C., Tamminga, C. A., Keshavan, M. S., Sweeney, J. A., Clementz, B. A., Hill, S. K., Pearlson, G., Yang, G., Creatura, G., Krystal, J. H., Repovs, G., Murray, J., Winkler, A., & Anticevic, A. (2019). Schizophrenia Exhibits Bi-directional Brain-Wide Alterations in Cortico-Striato-Cerebellar Circuits. *Cerebral Cortex*, *29*(11), 4463–4487. https://doi.org/10.1093/cercor/bhy306

Karahanoğlu, F. I., & Van De Ville, D. (2017). Dynamics of large-scale fMRI networks: Deconstruct brain activity to build better models of brain function. *Current Opinion in*

Biomedical Engineering, *3*, 28–36. https://doi.org/10.1016/j.cobme.2017.09.008

Kelly, R. M., & Strick, P. L. (2003). Cerebellar Loops with Motor Cortex and Prefrontal Cortex of a Nonhuman Primate. *The Journal of Neuroscience*, *23*(23), 8432–8444. https://doi.org/10.1523/JNEUROSCI.23-23-08432.2003

Kelly, R. M., & Strick, P. L. (2004). Macro-architecture of basal ganglia loops with the cerebral cortex: use of rabies virus to reveal multisynaptic circuits. In *Brain* (pp. 447–459). https://doi.org/10.1016/S0079-6123(03)43042-2

King, M., Hernandez-Castillo, C. R., Poldrack, R. A., Ivry, R. B., & Diedrichsen, J. (2019). Functional boundaries in the human cerebellum revealed by a multi-domain task battery. *Nature Neuroscience*, *22*(8), 1371–1378. https://doi.org/10.1038/s41593-019-0436-x

Latora, V., & Marchiori, M. (2001). Efficient Behavior of Small-World Networks. *Physical Review Letters*, *87*(19), 198701. https://doi.org/10.1103/PhysRevLett.87.198701

Lee, D., Seo, H., & Jung, M. W. (2012). Neural basis of reinforcement learning and decision making. *Annual Review of Neuroscience*, *35*, 287–308. https://doi.org/10.1146/annurev-neuro-062111-150512

MacLean, P. D. (1988). Evolution of Audiovocal Communication as Reflected by the Therapsid-Mammalian Transition and the Limbic Thalamocingulate Division. In *The Physiological Control of Mammalian Vocalization* (pp. 185–201). Springer US. https://doi.org/10.1007/978-1-4613-1051-8_11

Mavroudis, I. A., Petrides, F., Manani, M., Chatzinikolaou, F., Ciobică, A. S., Pădurariu, M., Kazis, D., Njau, S. N., Costa, V. G., & Baloyannis, S. J. (2017). Purkinje cells pathology in schizophrenia. A morphometric approach. *Romanian Journal of Morphology and Embryology = Revue Roumaine de Morphologie et Embryologie*, *58*(2), 419–424.

http://www.ncbi.nlm.nih.gov/pubmed/28730225

Mayka, M. A., Corcos, D. M., Leurgans, S. E., & Vaillancourt, D. E. (2006). Three-dimensional locations and boundaries of motor and premotor cortices as defined by functional brain imaging: A meta-analysis. *NeuroImage*, *31*(4), 1453–1474. https://doi.org/10.1016/j.neuroimage.2006.02.004

Mehler-Wex, C., Riederer, P., & Gerlach, M. (2006). Dopaminergic dysbalance in distinct basal ganglia neurocircuits: Implications for the pathophysiology of parkinson's disease, schizophrenia and attention deficit hyperactivity disorder. *Neurotoxicity Research*, *10*(3–4), 167–179. https://doi.org/10.1007/BF03033354

Meszlényi, R. J., Hermann, P., Buza, K., Gál, V., & Vidnyánszky, Z. (2017). Resting State fMRI Functional Connectivity Analysis Using Dynamic Time Warping. *Frontiers in Neuroscience*, *11*(FEB), 1–17. https://doi.org/10.3389/fnins.2017.00075

Neta, M., Schlaggar, B. L., & Petersen, S. E. (2014). Separable responses to error, ambiguity, and reaction time in cingulo-opercular task control regions. *NeuroImage*, *99*, 59–68. https://doi.org/10.1016/j.neuroimage.2014.05.053

Neychev, V. K., Fan, X., Mitev, V. I., Hess, E. J., & Jinnah, H. A. (2008). The basal ganglia and cerebellum interact in the expression of dystonic movement. *Brain*, *131*(9), 2499–2509. https://doi.org/10.1093/brain/awn168

Pelzer, E. A., Hintzen, A., Goldau, M., von Cramon, D. Y., Timmermann, L., & Tittgemeyer, M. (2013). Cerebellar networks with basal ganglia: feasibility for tracking cerebello-pallidal and subthalamo-cerebellar projections in the human brain. *European Journal of Neuroscience*, *38*(8), 3106–3114. https://doi.org/10.1111/ejn.12314

Ramnani, N., Behrens, T. E. J., Johansen-Berg, H., Richter, M. C., Pinsk, M. A., Andersson, J. L.

R., Rudebeck, P., Ciccarelli, O., Richter, W., Thompson, A. J., Gross, C. G., Robson, M. D., Kastner, S., & Matthews, P. M. (2006). The Evolution of Prefrontal Inputs to the Cortico-pontine System: Diffusion Imaging Evidence from Macaque Monkeys and Humans. *Cerebral Cortex*, *16*(6), 811–818. https://doi.org/10.1093/cercor/bhj024

Riedel, M. C., Ray, K. L., Dick, A. S., Sutherland, M. T., Hernandez, Z., Fox, P. M., Eickhoff, S. B., Fox, P. T., & Laird, A. R. (2015). Meta-analytic connectivity and behavioral parcellation of the human cerebellum. *NeuroImage*, *117*, 327–342. https://doi.org/10.1016/j.neuroimage.2015.05.008

Rottschy, C., Langner, R., Dogan, I., Reetz, K., Laird, A. R., Schulz, J. B., Fox, P. T., & Eickhoff, S. B. (2012). Modelling neural correlates of working memory: A coordinate-based meta-analysis. *NeuroImage*, *60*(1), 830–846. https://doi.org/10.1016/j.neuroimage.2011.11.050

Rubinov, M., & Sporns, O. (2010). Complex network measures of brain connectivity: Uses and interpretations. *NeuroImage*, *52*(3), 1059–1069. https://doi.org/10.1016/j.neuroimage.2009.10.003

Salmi, J., Pallesen, K. J., Neuvonen, T., Brattico, E., Korvenoja, A., Salonen, O., & Carlson, S. (2010). Cognitive and Motor Loops of the Human Cerebro-cerebellar System. *Journal of Cognitive Neuroscience*, *22*(11), 2663–2676. https://doi.org/10.1162/jocn.2009.21382

Schmahmann, J. D. (2019). The cerebellum and cognition. *Neuroscience Letters*, *688*(April 2018), 62–75. https://doi.org/10.1016/j.neulet.2018.07.005

Schmidt, L., D'Arc, B. F., Lafargue, G., Galanaud, D., Czernecki, V., Grabli, D., Schüpbach, M., Hartmann, A., Lévy, R., Dubois, B., & Pessiglione, M. (2008). Disconnecting force from money: effects of basal ganglia damage on incentive motivation. *Brain*, *131*(5), 1303–1310.

https://doi.org/10.1093/brain/awn045

Sgambato-Faure, V., Worbe, Y., Epinat, J., Féger, J., & Tremblay, L. (2016). Cortico-basal ganglia circuits involved in different motivation disorders in non-human primates. *Brain Structure and Function*, *221*(1), 345–364. https://doi.org/10.1007/s00429-014-0911-9

Sheffield, J. M., Kandala, S., Burgess, G. C., Harms, M. P., & Barch, D. M. (2016). Cingulo-opercular Network Efficiency Mediates the Association Between Psychotic-like Experiences and Cognitive Ability in the General Population. *Biological Psychiatry: Cognitive Neuroscience and Neuroimaging*, *1*(6), 498–506. https://doi.org/10.1016/j.bpsc.2016.03.009

Smeets, W. J. A. J., Marín, O., & González, A. (2000). Evolution of the basal ganglia: New perspectives through a comparative approach. *Journal of Anatomy*, *196*(4), 501–517. https://doi.org/10.1017/S0021878299006007

Sporns, O., Chialvo, D., Kaiser, M., & Hilgetag, C. (2004). Organization, development and function of complex brain networks. *Trends in Cognitive Sciences*, *8*(9), 418–425. https://doi.org/10.1016/j.tics.2004.07.008

Stein, J. L., Wiedholz, L. M., Bassett, D. S., Weinberger, D. R., Zink, C. F., Mattay, V. S., & Meyer-Lindenberg, A. (2007). A validated network of effective amygdala connectivity. *NeuroImage*, *36*(3), 736–745. https://doi.org/10.1016/j.neuroimage.2007.03.022

Stephan, H., & Andy, O. J. (1964). Quantitative Comparisons of Brain Structures from Insectivores to Primates. *American Zoologist*, *4*(1), 59–74.

Stephenson-Jones, M., Ericsson, J., Robertson, B., & Grillner, S. (2012). Evolution of the basal ganglia: Dual-output pathways conserved throughout vertebrate phylogeny. *The Journal of Comparative Neurology*, *520*(13), 2957–2973. https://doi.org/10.1002/cne.23087

Stoodley, C. J., & Limperopoulos, C. (2016). Structure–function relationships in the developing cerebellum: Evidence from early-life cerebellar injury and neurodevelopmental disorders. *Seminars in Fetal and Neonatal Medicine*, *21*(5), 356–364. https://doi.org/10.1016/j.siny.2016.04.010

Stoodley, C. J., Valera, E. M., & Schmahmann, J. D. (2012). Functional topography of the cerebellum for motor and cognitive tasks: An fMRI study. *NeuroImage*, *59*(2), 1560–1570. https://doi.org/10.1016/j.neuroimage.2011.08.065

Van Essen, D. C., Ugurbil, K., Auerbach, E., Barch, D., Behrens, T. E. J., Bucholz, R., Chang, A., Chen, L., Corbetta, M., Curtiss, S. W., Della Penna, S., Feinberg, D., Glasser, M. F., Harel, N., Heath, A. C., Larson-Prior, L., Marcus, D., Michalareas, G., Moeller, S., … Yacoub, E. (2012). The Human Connectome Project: A data acquisition perspective. *NeuroImage*, *62*(4), 2222–2231. https://doi.org/10.1016/j.neuroimage.2012.02.018

Von der Gablentz, J., Tempelmann, C., Münte, T. F., & Heldmann, M. (2015). Performance monitoring and behavioral adaptation during task switching: An fMRI study. *Neuroscience*, *285*, 227–235. https://doi.org/10.1016/j.neuroscience.2014.11.024

Walther, S., Stegmayer, K., Federspiel, A., Bohlhalter, S., Wiest, R., & Viher, P. V. (2017). Aberrant hyperconnectivity in the motor system at rest is linked to motor abnormalities in schizophrenia spectrum disorders. *Schizophrenia Bulletin*, *43*(5), 982–992. https://doi.org/10.1093/schbul/sbx091

Ward, P., Seri And, S., & Cavanna, A. E. (2013). Functional neuroanatomy and behavioural correlates of the basal ganglia: Evidence from lesion studies. *Behavioural Neurology*, *26*(4), 219–223. https://doi.org/10.3233/BEN-2012-120264

Whitfield-Gabrieli, S., & Nieto-Castanon, A. (2012). Conn : A Functional Connectivity Toolbox

for Correlated and Anticorrelated Brain Networks. *Brain Connectivity*, *2*(3), 125–141. https://doi.org/10.1089/brain.2012.0073

Wolpert, D. M., Diedrichsen, J., & Flanagan, J. R. (2011). Principles of sensorimotor learning. *Nature Reviews Neuroscience*, *12*(12), 739–751. https://doi.org/10.1038/nrn3112

Wu, T., & Hallett, M. (2013). The cerebellum in Parkinson's disease. *Brain*, *136*(3), 696–709. https://doi.org/10.1093/brain/aws360

Yin, H. H., Ostlund, S. B., & Balleine, B. W. (2008). Reward-guided learning beyond dopamine in the nucleus accumbens: the integrative functions of cortico-basal ganglia networks. *European Journal of Neuroscience*, *28*(8), 1437–1448. https://doi.org/10.1111/j.1460-9568.2008.06422.x

Supplemental Text

1. 100610, 101309, 102614, 102715, 102816, 103111, 103818, 104012, 104416, 105014, 105115, 105216, 105620, 105923, 106016, 106824, 107422, 108020, 108121, 108323, 108525, 109325, 109830, 111009, 111312, 111413, 111716, 112314, 112516, 112920, 113215, 113922, 114621, 114823, 114924, 115017, 116726, 117122, 118124, 118730, 118831, 119126, 119732, 119833, 120414, 120515, 121416, 122317, 122620, 123521, 123925, 124422, 125222, 126426, 126628, 127630, 127832, 128026, 128632, 128935, 129028, 129331, 129634, 130114, 130316, 130417, 130619, 130821, 131217, 132017, 132118, 133019, 133928, 134223, 134627, 135225, 136833, 137027, 137532, 138130, 138332, 138837, 140319, 143426, 144125, 144832, 145127, 146129, 146533, 149741, 149842, 150423, 151324, 151425, 151728, 151930, 152427, 153126, 153227, 153833, 154229, 154734, 156031, 156233, 156334, 156536, 157437, 157942, 159239, 159744, 161630, 162228, 162733, 163432, 164030, 164131, 164939, 167036, 167440, 168139, 169545, 172029, 172332, 172433, 172534, 173435, 173738, 173940, 174841, 175742, 176542, 177241, 178142, 178849, 178950, 179245, 180230, 180533, 180735, 180836, 182739, 182840, 185442, 185846, 186040, 188145, 189349, 189450, 190031, 191033, 192136, 195041, 195647, 196346, 198249, 198855, 199352, 202113, 204016, 204420, 206323, 206727, 208125, 211114, 211316, 212015, 212217, 213522, 214423, 219231, 220721, 236130, 245333, 275645, 281135, 285446, 286650, 287248, 299760, 304020, 309636, 310621, 311320, 314225, 316633, 321323, 329844, 336841, 349244, 350330, 358144, 361941, 381543, 385046, 391748, 397154, 397760, 414229, 419239, 459453, 468050, 510225, 516742, 529549, 529953, 547046, 552241, 561949, 567759, 571144, 580751, 589567, 618952, 622236, 675661, 680250, 680452, 748662, 757764, 789373, 835657, 849264, 97998

2. Data were collected on two different days. Each scanning session consisted of two 15-minute scans, resulting in four 15-minute scans total. The runs in each session were averaged together and the connectivity matrices for each session were contrasted against one another at a group-level using CONN. A false discovery rate correction was applied. No differences were found between the two sessions, indicating stable network connectivity patterns across sessions, even when data are collected on different days, *ps* > .9.

Supplemental Table 1. Abbreviations, region names, MNI coordinates, network association, and source for each ROIs used in the analyses. All ROIs are 3.5mm, spherical, and binarized. ROIs with the source "*Mirrored"* were created using its contralateral pair.

Abbreviation	Region	MNI (X, Y, Z)	Network	Source
L VSi	Left inferior ventral striatum	- 9, 9, -8	CCB-BG	Hausman, Jackson et al., 2019
R VSi	Right inferior ventral striatum	9, 9, -8	CCB-BG	*Mirrored*
L VSs	Left superior ventral striatum	-10, 15, 0	CCB-BG	Hausman, Jackson et al., 2019
R VSs	Right superior ventral striatum	10, 15, 0	CCB-BG	*Mirrored*
L DC	Left dorsal caudate	-13, 15, 9	CCB-BG	Hausman, Jackson et al., 2019
R DC	Right dorsal caudate	13, 15, 9	CCB-BG	*Mirrored*
L VRP	Left ventral rostral putamen	-20, 12, -3	CCB-BG	Hausman, Jackson et al., 2019
R VRP	Right ventral rostral putamen	20, 12, -3	CCB-BG	*Mirrored*
R CrusI	Right Cerebellar CrusI	47, -61, -34	CCB-BG	Hausman, Jackson et al., 2019
L Crus I	Left Cerebellar CrusI	-47, -61, -34	CCB-BG	*Mirrored*
R CrusII	Right Cerebellar CrusII	41, -70, -46	CCB-BG	Hausman, Jackson et al., 2019
L CrusII	Left Cerebellar CrusII	-41, -70, -46	CCB-BG	*Mirrored*
L DCP	Left dorsal caudal putamen	-28, 1, 3	MCB-BG	Hausman, Jackson et al., 2019
R DCP	Right dorsal caudal putamen	28, 1, 3	MCB-BG	*Mirrored*
L DRP	Left dorsal rostral putamen	-25, 8, 6	MCB-BG	Hausman, Jackson et al., 2019
R DRP	Right dorsal rostral putamen	25, 8, 6	MCB-BG	*Mirrored*
R LobV	Right Cerebellar Lobule V	16, -52, -17	MCB-BG	Hausman, Jackson et al., 2019
L LobV	Left Cerebellar Lobule V	-16, -52, -17	MCB-BG	*Mirrored*
R LobVI	Right Cerebellar Lobule VI	26, -60, -25	MCB-BG	Hausman, Jackson et al., 2019
L LovVI	Left Cerebellar Lobule VI	-26, -60, -25	MCB-BG	*Mirrored*
L dlPFC	Left dorsolateral prefrontal cortex	-43, 22, 34	FPN	Fair et al., 2009
R dlPFC	Right dorsolateral prefrontal cortex	43, 22, 34	FPN	Fair et al., 2009
L FG	Left frontal gyrus	-41, 3, 36	FPN	Fair et al., 2009
R FG	Right frontal gyrus	41, 3, 36	FPN	Fair et al., 2009
mCC	Medial cingulate cortex	0, 29, 30	FPN	Fair et al., 2009
L IPL	Left inferior parietal lobule	-51, -51, 36	FPN	Fair et al., 2009
R IPL	Right inferior parietal lobule	51, -47, 42	FPN	Fair et al., 2009
L IPS	Left intraparietal sulcus	-31, -59, 42	FPN	Fair et al., 2009
R IPS	Right intraparietal sulcus	30, -61, 39	FPN	Fair et al., 2009
L Precun	Left precuneus	-9, -72, 37	FPN	Fair et al., 2009
R Precun	Right precuneus	10, -69, 39	FPN	Fair et al., 2009
L aPFC	Left anterior prefrontal cortex	-28, 51, 1	CON	Fair et al., 2009
R aPFC	Right anterior prefrontal cortex	27, 50, 23	CON	Fair et al., 2009
L aI	Left anterior insula	-35, 14, 5	CON	Fair et al., 2009

R aI	Right anterior insula	36, 16, 4	CON	Fair et al., 2009
dACC	Dorsal anterior cingulate cortex	-1, 10, 46	CON	Fair et al., 2009
L aTh	Left anterior Thalamus	-12, -15, 7	CON	Fair et al., 2009
R aTh	Right anterior Thalamus	10, -15, 8	CON	Fair et al., 2009
amPFC	Anterior medial prefrontal cortex	1, 54, 21	DMN	Fair et al., 2009
vmPFC	Ventromedial prefrontal cortex	-3, 29, -2	DMN	Fair et al., 2009
L SFC	Left superior frontal cortex	-14, 38, 52	DMN	Fair et al., 2009
R SFC	Right superior frontal cortex	17, 37, 52	DMN	Fair et al., 2009
L ITL	Left inferior temporal lobe	-61, -33, -15	DMN	Fair et al., 2009
R ITL	Right inferior temporal lobe	65, -17, -15	DMN	Fair et al., 2009
L Para(DMN)	Left parahippocampus	-22, -26, -16	DMN	Fair et al., 2009
R Para(DMN)	Right parahippocampus	25, -26, -14	DMN	Fair et al., 2009
pCC	Posterior cingulate cortex	-2, -36, 37	DMN	Fair et al., 2009
L lPC	Left lateral parietal cortex	-47, -67, 36	DMN	Fair et al., 2009
R lPC	Right lateral parietal cortex	53, -67, 36	DMN	Fair et al., 2009
retsplen	Retro Splenial	3, 51, 8	DMN	Fair et al., 2009
supCC	Supragenual cingulate	0, 34, 30	EN	Stein et al., 2007
subCC	Subgenual cingulate	0, 15, -14	EN	Stein et al., 2007
L OFC	Left orbitofrontal cortex	-46, 31, -9	EN	Stein et al., 2007
R OFC	Right orbitofrontal cortex	46, 31, -9	EN	*Mirrored*
L Para(EN)	Left parahippocampus gyrus	-26, -19, -14	EN	Stein et al., 2007
L Para(EN)	Right parahippocampus gyrus	26, -19 -14	EN	*Mirrored*
L lPFC	Left lateral prefrontal cortex	-56, 26, 25	EN	Stein et al., 2007
R lPFC	Right lateral prefrontal cortex	56, 26, 25	EN	*Mirrored*
L Amyg	Left amygdala	-26, 0, -20	EN	Stein et al., 2007
R Amyg	Right amygdala	26, 0, -20	EN	*Mirrored*
pCC	Posterior cingulate cortex	0, -33, 38	EN	Stein et al., 2007
L vaI	Left ventral anterior insula	-33, 13, -7	EN	Deen et al., 2011
R vaI	Right ventral anterior insula	32, 10, -6	EN	Deen et al., 2011
mPMC	Mesial prefrontal cortex	-3 -5 60	MN	Mayka et al., 2006
pSMA	pre-supplementary motor area	-4 3 59	MN	Mayka et al., 2006
SMA	Supplementary motor area	-3 -11 61	MN	Mayka et al., 2006
L lPMC	Left lateral premotor cortex	-26 -10 62	MN	Mayka et al., 2006
R lPMC	Right lateral premotor cortex	25, -11, 61	MN	*Mirrored*
L dlPMC	Left dorsolateral premotor cortex	-30 -8 64	MN	Mayka et al., 2006
R dlPMC	Right dorsolateral premotor cortex	29 -9 64	MN	*Mirrored*
L vlPMC	Left ventral lateral premotor cortex	-52 7 22	MN	Mayka et al., 2006
R vlPMC	Right ventral lateral premotor cortex	52 6 21	MN	*Mirrored*
L SMC	Left sensorimotor cortex	-39 -24 59	MN	Mayka et al., 2006
R SMC	Right sensorimotor cortex	38 -25 59	MN	*Mirrored*

L M1	Left primary motor cortex	-37 -25 64	MN	Mayka et al., 2006
R M1	Right primary motor cortex	36 -21 58	MN	*Mirrored*
L S1	Left primary sensorimotor cortex	-40 -27 54	MN	Mayka et al., 2006
R S1	Right primary sensorimotor cortex	39 -28 54	MN	*Mirrored*
R Ling	Lingual_R	18, -47, -10	VN	Cassady et al., 2019
R Ling	Lingual_R	20, -66, 2	VN	Cassady et al., 2019
R Ling	Lingual_R	20, -86, -2	VN	Cassady et al., 2019
L Ling	Lingual_L	-15, -72, -8	VN	Cassady et al., 2019
L Ling	Lingual_L	-16, -52, -1	VN	Cassady et al., 2019
R Cal	Calcarine_R	8, -72, 11	VN	Cassady et al., 2019
R Cal	Calcarine_R	6, -81, 6	VN	Cassady et al., 2019
L Cal	Calcarine_L	-18, -68, 5	VN	Cassady et al., 2019
L Cal	Calcarine_L	-8, -81, 7	VN	Cassady et al., 2019
R Cun	Cuneus_R	15, -77, 31	VN	Cassady et al., 2019
R Cun	Cuneus_R	6, -72, 24	VN	Cassady et al., 2019
L Cun	Cuneus_L	-16, -77, 34	VN	Cassady et al., 2019
L Cun	Cuneus_L	-3, -81, 21	VN	Cassady et al., 2019
R Fus	Fusiform_R	27, -59, -9	VN	Cassady et al., 2019
L Fus	Fusiform_L	-33, -79, -13	VN	Cassady et al., 2019
R SupOcc	Occipital_Sup_R	15, -87, 37	VN	Cassady et al., 2019
R SupOcc	Occipital_Sup_R	24, -87, 24	VN	Cassady et al., 2019
L SupOcc	Occipital_Sup_L	-14, -91, 31	VN	Cassady et al., 2019
R MidOcc	Occipital_Mid_R	40, -72, 14	VN	Cassady et al., 2019
R MidOcc	Occipital_Mid_R	29, -77, 25	VN	Cassady et al., 2019
R MidOcc	Occipital_Mid_R	37, -81, 1	VN	Cassady et al., 2019
R MidOcc	Occipital_Mid_R	37, -84, 13	VN	Cassady et al., 2019
L MidOcc	Occipital_Mid_L	-40, -88, -6	VN	Cassady et al., 2019
L MidOcc	Occipital_Mid_L	-28, -79, 19	VN	Cassady et al., 2019
L MidOcc	Occipital_Mid_L	-24, -91, 19	VN	Cassady et al., 2019
L MidOcc	Occipital_Mid_L	-42, -74, 0	VN	Cassady et al., 2019
L MidOcc	Occipital_Mid_L	-26, -90, 3	VN	Cassady et al., 2019
R InfOcc	Occipital_Inf_R	43, -78, -12	VN	Cassady et al., 2019
L InfOcc	Occipital_Inf_L	-47, -76, -10	VN	Cassady et al., 2019
R InfTemp	Temporal_Inf_R	42, -66, -8	VN	Cassady et al., 2019
L InfTemp	Temporal_Inf_L	-42, -76, -10	VN	*Mirrored*
R Hes	Heschl_R	32, -26, 13	AN	Cassady et al., 2019
L Hes	Heschl_L	-30, -27, 12	AN	Cassady et al., 2019
L Hes	Heschl_L	-55, -9, 12	AN	Cassady et al., 2019
R Sup Temp	Temporal_Sup_R	65, -33, 20	AN	Cassady et al., 2019
R Sup Temp	Temporal_Sup_R	58, -16, 7	AN	Cassady et al., 2019

L Sup Temp	Temporal_Sup_L	-60, -25, 14	AN	Cassady et al., 2019
L Sup Temp	Temporal_Sup_L	-49, -26, 5	AN	Cassady et al., 2019
R RolOp	Rolandic_Oper_R	43, -23, 20	AN	Cassady et al., 2019
R RolOp	Rolandic_Oper_R	56, -5, 13	AN	Cassady et al., 2019
L RolOp	Rolandic_Oper_L	-38, -33, 17	AN	Cassady et al., 2019
R SupMar	SupraMarginal_R	59, -17, 29	AN	Cassady et al., 2019
L SupMar	SupraMarginal_L	-50, -34, 26	AN	Cassady et al., 2019
L SupMar	SupraMarginal_L	-53, -22, 23	AN	Cassady et al., 2019

Supplemental Table 2. All lateralized ROIs without a contralateral match were mirrored in the x direction. The following statistics are partial Pearson's correlation coefficients measuring the association between the GE of CB-BG networks and each affected network using only original ROIs (no mirrored).

	EN	MN	VN
CCB-BG	.16*	.18**	.10
MCB-BG	.03	.12	.28***

Note: Analyses were assessed using FDR correction. *** $p < .001$ ** $p < .01$ * $p < .05$

Supplemental Table 3. Pearson Correlation Coefficients (*r*) showing the relationship between each cortical network's global efficiency.

	FPN	CON	DMN	EN	MN	VN	AN
FPN	1	.21**	.19**	.13	.14*	.17*	.25***
CON	.21**	1	.27***	.20**	.30***	.28***	.35***
DMN	.19**	.27***	1	.25***	.31***	.27***	.25***
EN	.13	.20**	.25***	1	.24***	.20**	.25***
MN	.14*	.30***	.31***	.24***	1	.39***	.39***
VN	.17*	.28***	.27***	.20**	.39***	1	.40***
AN	.25***	.35***	.25***	.25***	.39***	.40***	1

Note: Analyses were assessed using FDR correction. *** $p < .001$ ** $p < .01$ * $p < .05$